Stable Transport of Assemblies by Pushing

Jay D. Bernheisel, *Student Member, IEEE*, and Kevin M. Lynch, *Senior Member, IEEE*

***Abstract*—This paper presents a method to determine whether an assembly of planar parts will stay assembled as it is pushed over a support surface. For a given pushing motion, an assembly is classified into one of three categories: (P = possible): any force necessary to preserve the assembly can be generated by the pushing contacts; (I = impossible): pushing forces cannot preserve the assembly; and (U = undecided): pushing forces may or may not be able to preserve the assembly. This classification is made based on the solution of linear constraint satisfaction problems. If the part–part and part–pusher contacts are frictionless, motions labeled P are guaranteed to preserve the assembly. The results are based on bounds on the possible support friction acting on individual parts in the face of indeterminacy in the distribution of support forces. Experimental results supporting the analysis are given.**

***Index Terms*—Assemblies, friction, linear constraint satisfaction, stable pushing, wrench space.**

I. Introduction

THE planar assembly of Fig. 1 is pushed over a horizontal support plane by its partially constraining fixture. Will the assembly be preserved and remain fixed to the fixture during the motion or will it fall apart or move relative to the fixture?

This paper addresses questions such as this by testing if the support frictional forces acting on the parts, due to sliding over the plane, act to close the partial kinematic constraints provided by the contacts between the pusher and the parts and among the parts themselves. If there is friction at the pusher–part and part–part contacts, then the set of possible constraint forces at the contacts increases, and the set of motions of the pusher that preserve the assembly may increase.

The problem of determining assembly-preserving pushing motions is a member of a class of problems we call *stable transport problems*. Although the term "stable" can be used with different meanings in a number of different contexts, in this paper, a "stable" motion simply means that the assembly is preserved and fixed to the fixture. (Discussion of other interpretations is left to Section VIII.) Examples of stable transport problems include determining if an assembly will be preserved under a particular motion of the fixture, finding the set of assembly-preserving motions, using these motions to plan fast or short paths for the assembly between configurations, and designing the fixture to facilitate stable motion. Different formulations of these problems may include inertial forces of the parts, gravity, and/or sliding friction over constraint surfaces such as a support plane. We are motivated by the possibility of using a low-degree-of-freedom manipulator to manipulate several parts simultaneously, perhaps also taking advantage of environmental constraints (e.g., a support surface) to reduce manipulator size, strength, and dexterity requirements. Stable transport problems also arise in parts-handling, manufacturing tasks, and automated packaging tasks.

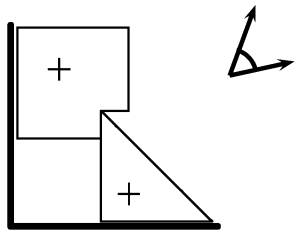

Fig. 1. If the frictionless L-shaped pusher translates in one of the directions indicated, the assembly will be preserved during motion.

This paper provides the most complete answers to date on problems of stable pushing. Under the assumptions of quasi-static motion and planar contact, this paper addresses, for the first time, to the best of the authors' knowledge, the stability of arbitrary assemblies of parts during pushing. This analysis is complicated by the quasi-statically indeterminate distribution of support forces acting on each part, which yields uncertainty in the support friction wrench (resultant force and torque) acting on the part. We provide methods to bound this uncertainty based on the known center of mass (CM) of the part and its geometry. With these bounds, a pushing motion is either labeled P (stable push is possible), meaning that any force necessary to preserve the assembly can be generated by the pushing contacts, I (stable push is impossible), meaning that pushing forces cannot preserve the assembly, or U (undecided, neither P nor I), pushing forces may or may not be able to preserve the assembly.

We provide algorithms to classify all possible pushing motions into the categories P, I, or U and provide results of an experiment in pushing an assembly. This paper extends our previous work on pushing a linear stack of parts [4], [5]. The algorithms in that work found pushing motions guaranteeing stability, but applied only to a single straight-edge pusher pushing a linear stack of parts with edge–edge contact between parts. In this paper, we allow arbitrary assemblies, including loops and trees of parts. If the pusher–part and part–part contacts are frictionless, then pushing motions labeled P are guaranteed to be stable. If these contacts are not frictionless, then, due to frictional ambiguity issues, some motions labeled P may actually be unstable.

Manuscript received July 22, 2005. This paper was recommended for publication by Associate Editor J. Wen and Editor F. Park upon evaluation of the reviewers' comments. This work was supported by the National Science Foundation under Grant IIS-0308224. The work of J. D. Bernheisel was supported by the National Science Foundation through an IGERT Fellowship. This paper was presented in part at the 2005 International Conference on Robotics and Automation.

The authors are with the Mechanical Engineering Department, Northwestern University, Evanston, IL 60208 USA (e-mail: jay@bernheisel.org).

Digital Object Identifier 10.1109/TRO.2006.875488

A. Related Work

This paper follows directly in a line of work begun by Mason [15], who provided a rule for determining the rotation direction of a planar part pushed with point contact. This was followed by work by Peshkin and Sanderson [22] on bounding the speed of rotation. Lynch and Mason [11], [12] used these results to derive stable pushing motions for a single part pushed with edge–edge contact. This work was extended by Bernheisel and Lynch [4], [5] to a linear stack of parts, possibly with uncertainty in the parts' centers of mass. A similar problem was studied by Harada *et al.* [9].

Pushing single three-dimensional (3-D) parts has been studied by Mayeda and Wakatsuki [20]. The mechanics changes somewhat when including 3-D effects (e.g., pushing out of the plane moves the effective CM of the object). Maeda *et al.* [13], [14] constructed a single framework to consider several types of 3-D nonprehensile motion including 3-D pushing.

Also relevant to the work in this paper is past work on fixturing and formulating complementarity problems to solve for the motion of multiple parts in contact. We do not attempt to review this work here, but mention a few particularly relevant works. Our work solves linear constraint satisfaction problems to find feasible contact forces for a given motion of an assembly. Other work has used polyhedral convex cone intersection [1], linear programming [24], and linear matrix inequalities [7] to find contact forces for grasping or fixturing single parts. Yu *et al.* [25] solved a force balance for multiple parts grasped by point contacts to determine whether a stable grasp was possible. In that work, gravity was not considered, nor were any indeterminate external forces such as the sliding friction in our problem. Mattikalli *et al.* [19] provided linear programs to determine the stability of a frictionless assembly of polygons in gravity, and to find the "most stable" orientation of an unstable assembly. Mattikalli *et al.* [18] extended that work to find all unstable orientations of assemblies with friction. For multiple parts that can roll against each other and their manipulator without slipping, Harada *et al.* [8] demonstrated a control method that uses linear programming to ensure that the friction constraints are satisfied. Baraff *et al.* [3] proposed methods to design three different types of fixtures for frictionless assemblies of polyhedra. A fixture that provides *directional stability* balances a given external wrench exactly. A fixture that provides *robust directional stability* balances a given external wrench plus any small perturbation of that wrench. A *form-closure* fixture balances any external wrench. Mosemann *et al.* [21] computed stable orientations of frictional assemblies in uniform gravity.

B. Outline

Section II gives the definitions and assumptions used throughout the paper. Section III defines the types of pushing contacts considered in this paper. Conservative bounds on the possible support friction wrenches acting on a part are developed in Section IV. The intersection of the possible support and pushing wrenches determines whether or not a given motion could be stable. Algorithms for performing this intersection are described in Section V. Section VI gives results of the algorithms on example assemblies. Section VII reports the results of an experiment on stable pushing of an assembly. Finally, Section VIII discusses limitations and possible extensions to this work.

II. Definitions and Assumptions

Parts slide over a support plane normal to the gravity vector. The planar velocity of a part can be expressed as a 3-D twist $\mathbf{v} = [v_x, v_y, \omega_z]^T$, representing the two components of translational velocity and the single angular velocity in a frame fixed to the part, often chosen at the CM. This motion can also be expressed as a rotation center in the part frame, and $\mathrm{COR}(\mathbf{v})$ returns the center of rotation (COR) $(v_y/\omega_z, -v_x/\omega_z)$ in the part frame, as well as the sign of rotation $\mathrm{sgn}(\omega_z)$, for $\omega_z \neq 0$.

We assume all motion is quasi-static: the pushing forces applied to a part are equal and opposite the frictional forces the support surface applies to the part to resist its motion. There is no pushing force "left over" to accelerate the part. Coulomb friction governs the pushing contacts and the support contacts between the part and the surface. In particular, the support frictional forces are independent of the speed of motion $\|\mathbf{v}\|$ of the part. We use a static coefficient of friction for the pushing contacts and a kinetic coefficient of friction for the support friction. We also assume that the friction coefficient between each part and the surface is uniform over the part. We do not review the mechanics of quasi-static pushing here; see [15]–[17].

Both a pushing force and a support friction force acting on a part can be expressed as a 3-D wrench $\mathbf{w} = [f_x, f_y, \tau_z]^T$, representing the two linear forces and the single torque expressed in the part-fixed frame. Throughout this paper, we refer to a pushing contact force applied to a part as a *pushing wrench* $\mathbf{p} = [p_x, p_y, p_z]^T$. We refer to a frictional force *a part applies to the support surface* as a *support friction wrench* or simply *support wrench*, $\mathbf{s} = [s_x, s_y, s_z]^T$. During quasi-static motion, the pushing wrench and support wrench for a part are equal; by our definition, the support wrench is the negative of the wrench resisting motion.

The pushing wrench $\mathbf{p}$ acting on a part arises from part–part and pusher–part contact. In this paper we assume all such contacts can be modeled as point contacts with a unique inward normal acting on the parts. The friction coefficient μ at a point contact defines two lines of force through the contact at angles $\tan^{-1}\mu$ to the contact normal. These forces define the edges of the *friction cone*, and any wrench acting on the part due to this contact must be a nonnegative linear combination of these two forces and their torque components. The total pushing wrench acting on a part is the sum of the pushing wrenches at each of the contacts, and therefore it lies inside a polyhedral convex cone rooted at the origin of the part's wrench space (see Fig. 2).

The support wrench $\mathbf{s}$ is determined by the part motion direction $\mathbf{v}/\|\mathbf{v}\|$, the part mass m, the support friction coefficient μ_s, and the distribution of support normal forces over the part. Because the part may make more than three points of contact with the surface, and the contact points are unknown, the distribution of support forces is statically indeterminate. This means that the exact support wrench for a given part motion is fundamentally

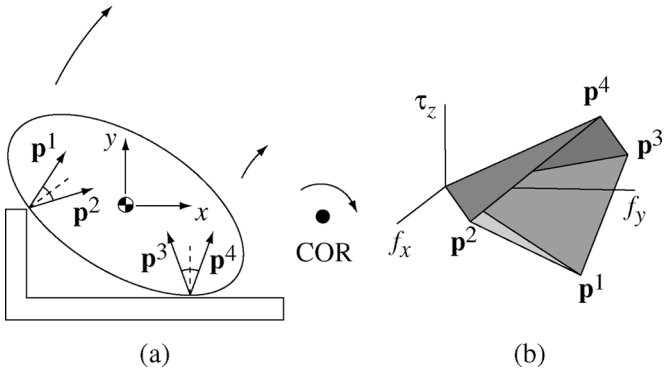

Fig. 2. (a) The part is being rotated about the COR by two pushing contacts. Each pushing contact defines a unique inward-pointing normal, and the friction coefficient defines a friction cone. The edges of the friction cones define unit wrenches $\mathbf{p}^1, \mathbf{p}^2, \mathbf{p}^3$, and $\mathbf{p}^4$. (b) The set of all possible pushing wrenches that can be applied to the part is the set of all nonnegative linear combinations of the friction cone edge pushing wrenches, defining a polyhedral cone in the part's wrench space.

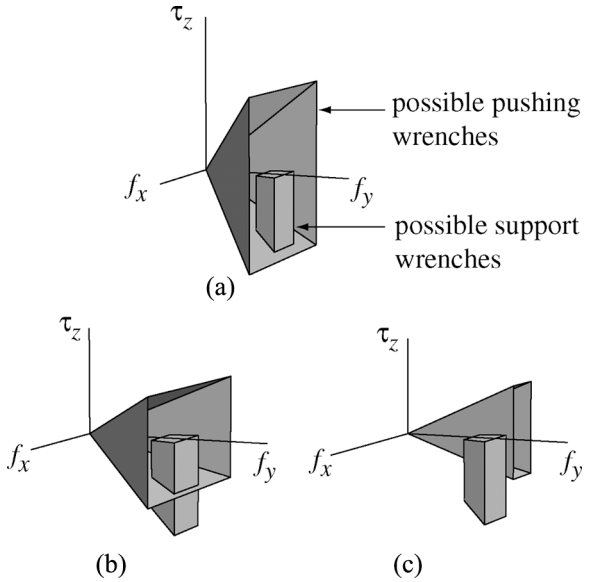

Fig. 3. For a given velocity $\mathbf{v}$ of a single sliding part, the possible support wrenches are represented by a closed region in the wrench space, while the pushing contact generates an infinite polyhedral convex cone of possible pushing wrenches, rooted at the origin. (a) The cone completely contains the possible support wrenches, so the pushing wrench cone can generate any wrench that would be needed to move the part with velocity $\mathbf{v}$. (b) The cone overlaps but does not contain the possible support wrenches, so the pushing wrench cone may or may not be able to generate the necessary wrench. (c) The cone does not overlap the support wrenches at all, meaning that the pushing contact cannot move the part with velocity $\mathbf{v}$.

unknowable. Nonetheless, as we show in Section IV, it is possible to place bounds on the set of possible support wrenches given the known geometry of the part and its CM. In the special case that the part is translating, this wrench set reduces to a single force of magnitude $\mu_s mg$, where g is gravitational acceleration, passing through the CM in the direction of translation [15]. We assume that the part's geometry, mass m, CM location, and support friction coefficient μ_s are known.

One question of interest in this paper is the following: given a motion of the pusher, will the part stay fixed relative to it? If it does, we call this a *stable* push. To answer this question, we first assume that the push is stable, meaning that the motion $\mathbf{v}$ of the part is known. We use this information to compute bounds on the part's support wrench. If every possible support wrench can be generated by the pushing contacts, then stable pushing of the part is a consistent solution. If none of the possible support wrenches can be generated, then the push is unstable.

Fig. 3 demonstrates this idea graphically. In Fig. 3(a), every possible support wrench can be generated by the contacts, so stable pushing can occur. In Fig. 3(c), none of the support wrenches can be generated, and the push is unstable. In Fig. 3(b), some of the possible support wrenches can be generated, so stable pushing cannot be ruled out. The possible support wrenches collapse to a single point for translations, so only the cases of Fig. 3(a) or (c) will apply.

In Fig. 3(a), we might be tempted to say that stable pushing is guaranteed to occur. This may not be the case, however, due to ambiguities in the solution of rigid-body mechanics problems with Coulomb friction [6], [10]. Other solutions to the part's motion may also be possible (see Fig. 4). If the pushing contacts are frictionless, however, then the frictional ambiguity problem goes away, and we can guarantee that the situation in Fig. 3(a) is stable.

Our primary interest in this paper is not stable pushing of a single part, but stable pushing of assemblies of parts. The classification in Fig. 3 holds also for multiple parts. For any possible combination of part support wrenches, there may exist pushing wrenches that can simultaneously generate them [e.g., Fig. 3(a)]; there may exist pushing wrenches that can only generate some of the possible support wrenches [e.g., Fig. 3(b)], or there may exist no combination of support wrenches that can be generated by the pushing wrenches [e.g., Fig. 3(c)]. To simplify the discussion, for the rest of the paper we refer to the case in Fig. 3(a) as P: a stable push is possible, meaning that all possible support wrenches can be generated by the pushing contacts. The case in Fig. 3(b) is referred to as U (undecided): the behavior of the assembly can not be predicted. The case in Fig. 3(c) is referred to as I: a stable push is impossible, as none of the possible combinations of support wrenches can be generated by the pushing contacts. Since there is no uncertainty in part support wrenches during translation, translational motions (rotation centers at infinity) are always labeled either P or I.

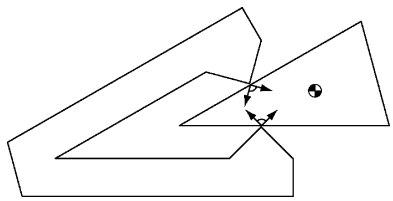

Fig. 4. Rigid jaw-shaped pusher makes two points of contact with the triangular part, and the possible pushing wrenches span the entire wrench space (i.e., force closure). Because of this, all pusher motions are labeled P—stable pushing is a consistent solution. If the pusher moves to the left, however, simply breaking contact is another consistent solution. The true answer is determined by whether the part is wedged into the pusher with significant internal forces not modeled in the rigid-body model.

III. Pushing Contacts

We assume that all part–part and pusher–part contacts in an assembly can be treated as a discrete set of point contacts,

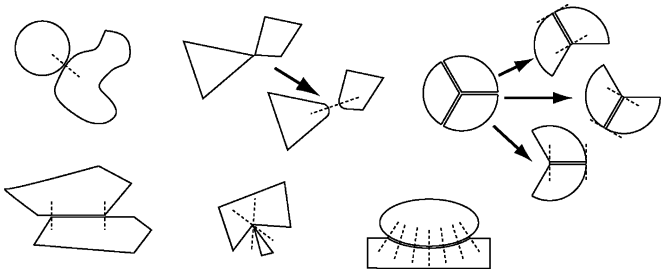

Fig. 5. Modeling contacts as point contacts with unique normals.

each with a friction coefficient and unique and opposite inward-pointing contact normals on each part in the contact. This allows modeling all vertex-edge contacts in a polygonal assembly. Polygonal edge–edge contacts are modeled as two point contacts at the ends of the common edge, provided the friction coefficient is constant along the edge. Convex vertex-vertex contacts are a degenerate case where a unique contact normal is not defined. Such contacts can be accounted for by infinitesimally "rounding the corners," providing a unique contact normal. Vertex–vertex contact is allowed if one of the vertices involved is concave; in this case, the contact is modeled as two point contacts with normals defined by the edges adjacent to the concave vertex. Contacts between smooth curves can also be represented by point contacts, except in the case that two nonlinear curves make contact for an extended length. In this case, the contact must be approximated by a set of points along the contact. All contacts involving more than two parts can be resolved into a set of pairwise contacts (see Fig. 5).

At a point contact between part i and part j, choose the contact normal pointing into part i, and let $\mathbf{p}^1$ and $\mathbf{p}^2$ be the unit wrenches of the friction cone edges pointing into part i. These wrenches are represented in a common reference frame for the two parts, not necessarily at the CM of either part. Then the wrench acting on part i due to the contact is $b^{i,1}\mathbf{p}^1 + b^{i,2}\mathbf{p}^2$, where $b^{i,1}, b^{i,2} \geq 0$. The wrench acting on part j is equal and opposite, i.e., $b^{j,1}\mathbf{p}^1 + b^{j,2}\mathbf{p}^2$, where $b^{j,1} = -b^{i,1}$ and $b^{j,2} = -b^{i,2}$. The total pushing wrench acting on a part is the sum of the pushing wrenches from all its part–part and pusher–part contacts.

IV. Support Wrenches for a Single Part

Let r be the distance from the part's CM to the most distant point of its support area. For the purposes of deriving conservative bounds on the possible support wrenches for a given motion of the part, we treat the part as a disk of radius r centered at its CM [22]. The set of possible support wrenches for the disk subsumes the set of possible support wrenches for the actual part.

Without loss of generality, assume that the COR is located at $(d, 0)$ in a part frame fixed to the CM, where $d > r$. We also assume that rotation is clockwise $(-)$; the case of counterclockwise rotation yields support wrenches opposite of those found here. The support friction wrench applied by the part to the support plane due to rotation about the COR is written $\mathbf{s} = [s_x, s_y, s_z]^T$. The exact support friction wrench is unknown, due to the static indeterminacy of the support. However,

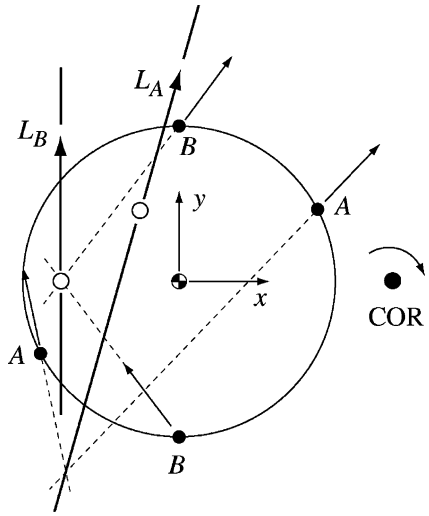

Fig. 6. The disk is rotating about the COR shown. Two cases are illustrated: the two support feet are either located at the points marked A or at the points marked B. For both cases, the support friction force magnitudes are equal at each foot and in the direction of motion of the foot. Summing the support forces, we get the line of force L_A for the case of feet at A and the line of force L_B for the case of feet at B. The $\mathrm{CF}_{\mathrm{eff}}$ for each case is the point on the line closest to the COR and is marked by a ◯.

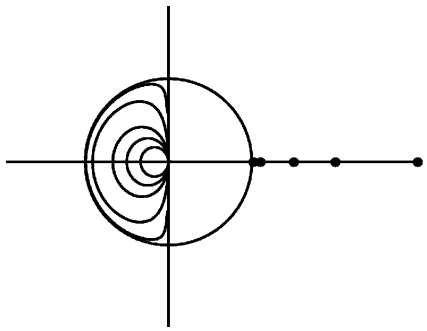

Fig. 7. As the COR moves out along the x-axis, the set of possible effective centers of friction shrinks. As the COR approaches infinity, the $\mathrm{CF}_{\mathrm{eff}}$ region approaches the single point at the CM.

we can use the conjecture described in [22] to find bounds on the set of possible support friction wrenches associated with the given COR. This "dipod method," which applies for $d > r$, models the support distribution as two points of support on the circumference of the disk, collinear with the CM, each with support force $mg/2$. As these two feet are rotated around the disk, we get a closed one-dimensional (1-D) curve of support wrenches.

To represent these support friction wrenches, note that any support wrench has a corresponding line of action in the plane. The unique point on the line closest to the COR is called the effective center of friction, or $\mathrm{CF}_{\mathrm{eff}}$ [11]. All support can be considered to be concentrated at the $\mathrm{CF}_{\mathrm{eff}}$ during the motion (see Fig. 6). The dipod method constructs a curve of $\mathrm{CF}_{\mathrm{eff}}$ with the property that the actual $\mathrm{CF}_{\mathrm{eff}}$ (for the unknown support distribution) must lie on or inside the curve (see Fig. 7). The curve shrinks to a point at the CM as the COR goes to infinity.

The $\mathrm{CF}_{\mathrm{eff}}$ bounds in Fig. 7, when combined with bounds on the magnitude of the support wrench, define a connected region of possible support wrenches in the part's wrench space. This

region is nonlinear. We would like to find a simple, conservative, convex approximation to this region described by linear constraints.

To find such an approximation, we derive three bounds: 1) bounds on the magnitude of the linear portion of the support wrench $\sqrt{(s_x)^2+(s_y)^2}$; 2) bounds on the moment-to-force ratio $s_z/\sqrt{(s_x)^2+(s_y)^2}$; and 3) bounds on the linear force angle $\operatorname{atan2}(s_y, s_x)$, where $\operatorname{atan2}(s_y, s_x)$ is the angle to the point (s_x, s_y) in the plane. These bounds allow us to approximate the true support wrench region by a six-sided polyhedron in the wrench space.

A. Bounds on Force Magnitude

When the part is translating, let $f_{\max} = \mu_s mg = \sqrt{(s_x)^2+(s_y)^2}$ be the magnitude of the linear portion of the support wrench. In other words, when the COR is at $(\infty, 0)$, the support wrench is $[0, f_{\max}, 0]^T$. This same support wrench is obtained for a COR at $(d, 0)$, $d > r$, for support feet at $(r, 0)$ and $(-r, 0)$. The support friction forces at each point of support are acting in the same direction, so there is no cancellation of forces, and the support force magnitude is maximal.

When the COR is at $(d, 0)$, where d is finite, the support friction vectors at each point of support may have some cancellation with each other, meaning that the total support friction magnitude may be less than $f_{\max}$. This cancellation is maximized when the support feet are at the points $(0, r)$ and $(0, -r)$. A simple calculation yields the lower bound in the following bounds on force magnitude:

$$\frac{f_{\max}}{\sqrt{1+\left(\frac{r}{d}\right)^2}} \leq \sqrt{(s_x)^2+(s_y)^2} \leq f_{\max}. \tag{1}$$

B. Bounds on Moment-to-Force Ratio

The magnitude of the ratio $s_z/\sqrt{(s_x)^2+(s_y)^2}$ is maximized when the support force is equally distributed at $(0, r)$ and $(0, -r)$ on the disk. In this case, the $\mathrm{CF}_{\mathrm{eff}}$ is located at $(-r^2/d, 0)$ in the part frame, and the line of action of the support force is parallel to the y-axis. Therefore, the torque about the CM is $s_z = -r^2\sqrt{(s_x)^2+(s_y)^2}/d$ (note that it is negative). The maximum torque is $s_z = 0$ for support feet at $(r, 0)$ and $(-r, 0)$. Our second set of bounds is

$$\frac{-r^2}{d} \leq \frac{s_z}{\sqrt{(s_x)^2+(s_y)^2}} \leq 0. \tag{2}$$

C. Bounds on Force Angle

Again using the dipods, if we set the angle from the CM to one foot of the dipod as β, then the two feet of the dipod are at $(r\cos\beta, r\sin\beta)$ and $(-r\cos\beta, -r\sin\beta)$. Thus, the vectors from the COR to the two feet are $(r\cos\beta - d, r\sin\beta)$ and $(-r\cos\beta - d, -r\sin\beta)$. Rotating these by $-90°$, the support forces at each foot are aligned with the vectors $\mathbf{f}_1 = (r\sin\beta, d - r\cos\beta)$ and $\mathbf{f}_2 = (-r\sin\beta, r\cos\beta + d)$. The angle $\phi(\beta)$ of the total support force is given by

$$\phi(\beta) = \frac{1}{2}\left(\operatorname{atan2}(\mathbf{f}_1) + \operatorname{atan2}(\mathbf{f}_2)\right)$$

where $\operatorname{atan2}(\mathbf{f})$ gives the angle in the plane of the vector $\mathbf{f}$. We then solve

$$\frac{d\phi}{d\beta} = 0$$

to find the values of β where the angle is maximized or minimized. This yields the four solutions

$$\beta = \pm\cos^{-1}\left(\pm\frac{\sqrt{r^2+d^2}}{d\sqrt{2}}\right)$$

with all four combinations of the "±." If we set both of the ±'s to be + and plug this solution into $\phi(\beta)$, we find that the minimum angle of the support force is

$$\alpha_{\min} = \frac{1}{2}\left[\operatorname{atan2}\left(d + \frac{r\sqrt{r^2+d^2}}{d\sqrt{2}}, -r\sqrt{1-\frac{r^2+d^2}{2d^2}}\right)\right] + \frac{1}{2}\left[\operatorname{atan2}\left(d - \frac{r\sqrt{r^2+d^2}}{d\sqrt{2}}, r\sqrt{1-\frac{r^2+d^2}{2d^2}}\right)\right].$$

Thus, our bounds on the angle of the support force are

$$\alpha_{\min} \leq \operatorname{atan2}(s_y, s_x) \leq \pi - \alpha_{\min} \tag{3}$$

due to symmetry.

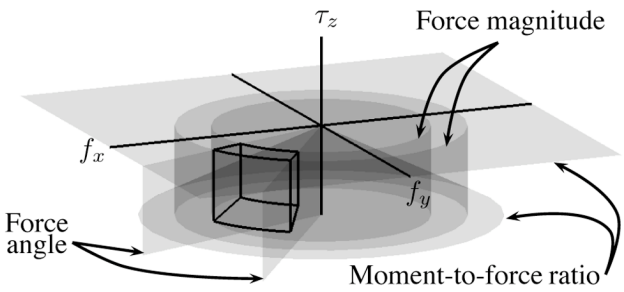

Fig. 8. Example support wrench region. The gray surfaces show the three sets of support wrench bounds and the six-sided region shows their intersection.

D. Combining the Bounds

Now, we can combine the bounds in wrench space to get a conservative approximation to the possible support wrenches. We want the convex hull of linear constraints to contain all possible support wrenches. The force magnitude bounds define two cylinders centered on the s_z-axis: the wrench must be outside one and inside the other. The bounds on the moment-to-force ratio, say s_z, must be negative but above a right circular cone. The force angle bounds say the wrenches must be in a pie wedge bounded by planes perpendicular to the $s_x - s_y$ plane (see Fig. 8).

This region is not a convex polyhedron in the wrench space due to the cylindrical force magnitude bounds and the cone moment-to-force bound. To find a six-sided convex polyhedron containing the region satisfying the constraints (1)–(3), we find the eight wrenches $\tilde{\mathbf{s}}^k$, $k = 1 \ldots 8$, at the "corners" of the region, obtained by the $2^3 = 8$ combinations of the equalities at the extremes of the three sets of constraints. The eight corners of our polyhedral convex approximation $\mathbf{s}^k$, $k = 1 \ldots 8$, are obtained from the $\tilde{\mathbf{s}}^k$ by taking the four wrenches $\tilde{\mathbf{s}}^k$ obtained with the upper bound on force magnitudes and multiplying them by $1/\sin(\alpha_{\min})$, while leaving the other four unchanged. This guarantees that the convex hull of the $\mathbf{s}^k$

$$\sum_{k=1}^{8} a^k \mathbf{s}^k, \quad \text{where } a^k \geq 0, \sum_{k=1}^{8} a^k = 1 \tag{4}$$

contains the original nonconvex region. This six-sided polyhedron will be our conservative approximation to the possible support wrenches for a given COR.

All of the mechanics of this section have assumed that the COR is along the part's x-axis. If this is not the case, then the analysis holds for the COR along an x'-axis, and we simply rotate the $\mathbf{s}^k$ by the same angle needed to rotate the x-axis to the x'-axis.

For convenience when comparing support wrenches to pushing wrenches, in Section V, support wrenches for a part are expressed in a common reference frame for the entire assembly and not the individual part frame.

V. Testing Stability of an Assembly

A pushed assembly consists of n parts and m point contacts. These pushing contacts give rise to $2m$ wrenches representing the unit wrenches at the friction cone edges $\mathbf{p}^j$, $j = 1 \ldots 2m$, expressed in a common world frame. The total pushing wrench acting on part i is

$$\sum_{j=1}^{2m} b^{i,j} \mathbf{p}^j$$

where $b^{i,j}$ is the weighting coefficient of the wrench $\mathbf{p}^j$ on part i. Since many of the wrenches do not act on a given part, many of these coefficients are zero. These coefficients take nonnegative values if the wrench was defined as "into" the part and nonpositive values if the wrench was defined as "away" from the part (i.e., into the other part in the contact). In addition, if $\mathbf{p}^j$ acts on parts i and k, then we have $b^{i,j} = -b^{k,j}$.

For a given motion of the assembly, each part i has a support wrench of the form

$$\sum_{k=1}^{8} a^{i,k} \mathbf{s}^{i,k}$$

where, as described in Section IV, each $\mathbf{s}^{i,k}$ is one of the eight corners of the support wrench region for part i, represented in the world frame, and each $a^{i,k} \geq 0$ is a weighting coefficient, with $\sum_{k=1}^{8} a^{i,k} = 1$.

We would like to know if the motion of the pusher falls into the category P (stable motion is a consistent solution for all possible support distributions) or I (stable motion is impossible for all possible support distributions). If neither of these is the case, the motion is labeled U. In Section V-A, we give an algorithm to determine if a given pushing motion is I. In Section V-B, we give an algorithm to determine if a given pushing motion is P. In Section V-C, we give a simplified algorithm to determine the translation directions labeled P.

A. Testing for Guaranteed Instability

For a given pushing motion of the assembly, if it is possible to choose part support wrenches (from their bounded uncertainty regions) and pushing wrenches such that there is force balance for all parts, then the motion is labeled P or U. If not, the motion is labeled I. For this problem, the design variables are the support wrench weights $a^{i,k}$ and the pushing wrench weights $b^{i,j}$, $i = 1, \ldots, n, j = 1, \ldots, 2m$, and $k = 1, \ldots, 8$.

To simplify the description of the linear constraint satisfaction problem, we introduce the following notation. For part i, define the column vector of support wrench weights $\mathbf{a}^i \in \mathbb{R}^8$ to be

$$\mathbf{a}^i = [a^{i,1}, \ldots, a^{i,8}]^T.$$

For a given part motion, define S^i to be the 3×8 matrix defining the corners of the support wrench region, which is obtained by placing the eight column vectors $\mathbf{s}^{i,k}$, $k = 1, \ldots, 8$, side by side

$$S^i = [\mathbf{s}^{i,1} \mathbf{s}^{i,2}, \ldots, \mathbf{s}^{i,8}].$$

Then, the support wrench for part i is given by the column vector $S^i \mathbf{a}^i \in \mathbb{R}^3$.

Now, define the column vector $\mathbf{a} \in \mathbb{R}^{8n}$ obtained by stacking the n vectors $\mathbf{a}^i$

$$\mathbf{a} = \left[(\mathbf{a}^1)^T \ (\mathbf{a}^2)^T \ \ldots \ (\mathbf{a}^n)^T \right]^T$$

and the $3n \times 8n$ block-diagonal matrix S built from the n 3×8 matrices S^i

$$S = \begin{bmatrix} S^1 & & \mathbf{0} \\ & \ddots & \\ \mathbf{0} & & S^n \end{bmatrix}.$$

Then, the column vector $S\mathbf{a} \in \mathbb{R}^{3n}$ represents the support wrenches of all n parts, where the first three elements represent the support wrench for part 1, and so on.

Similarly, for part i, define the pushing wrench weight vector

$$\mathbf{b}^i = [b^{i,1} \ b^{i,2} \ \ldots \ b^{i,2m}]^T \in \mathbb{R}^{2m}$$

multiplying the pushing wrenches $\mathbf{p}^j$, $j = 1 \ldots 2m$. Stacking the n column vectors $\mathbf{b}^i$, we get the $2mn$-length column vector

$$\mathbf{b} = \left[(\mathbf{b}^1)^T \ (\mathbf{b}^2)^T \ \ldots \ (\mathbf{b}^n)^T \right]^T.$$

Now, define the matrix P' to be the $3 \times 2m$ matrix obtained by lining up the column vectors $\mathbf{p}^j$, $j = 1 \ldots 2m$ side by side

$$P' = [\mathbf{p}^1 \ \mathbf{p}^2 \ \ldots \ \mathbf{p}^{2m}]$$

and the $3n \times 2mn$ block-diagonal matrix P with the matrices P' along the diagonal

$$P = \begin{bmatrix} P' & & \mathbf{0} \\ & \ddots & \\ \mathbf{0} & & P' \end{bmatrix}.$$

Then, the column vector $P\mathbf{b} \in \mathbb{R}^{3n}$ represents the pushing wrench on all n parts, where the first three elements represent the pushing wrench for part 1, and so on. To satisfy force balance for all the parts, the condition

$$S\mathbf{a} - P\mathbf{b} = \mathbf{0} \in \mathbb{R}^{3n}$$

must hold.

The design variables $\mathbf{a}$ and $\mathbf{b}$ are not unconstrained, however. The $\mathbf{a}$ vector must satisfy

$$C\mathbf{a} = [1, 1, \ldots, 1]^T \in \mathbb{R}^n$$

where the $n \times 8n$ matrix C is

$$C = \begin{bmatrix} \mathbf{1}_8 & \mathbf{0} & \ldots & \mathbf{0} \\ \mathbf{0} & \mathbf{1}_8 & \ldots & \mathbf{0} \\ & & \vdots & \\ \mathbf{0} & \ldots & \mathbf{0} & \mathbf{1}_8 \end{bmatrix}$$

where $\mathbf{1}_8$ is a row 8-vector of 1's. The elements of $\mathbf{a}$ are also constrained to be nonnegative, $\mathbf{a} \geq \mathbf{0}$. These constraints restrict each part's support wrench to the six-sided polyhedron determined in Section IV that conservatively approximates the possible support wrenches.

To satisfy the constraints on $\mathbf{b}$, we decompose it into three components: $\mathbf{b}_0$, the coefficients that must be zero; $\mathbf{b}_+$, the coefficients that must be nonnegative; and $\mathbf{b}_-$, the coefficients that must be nonpositive. Thus, perhaps after permuting the elements of the P matrix, the vector $\mathbf{b}$ can be written $\mathbf{b} = [\mathbf{b}_0^T \ \mathbf{b}_+^T \ \mathbf{b}_-^T]^T$. The dimensions of $\mathbf{b}_+$ and $\mathbf{b}_-$ are equal, and they must satisfy

$$\mathbf{b}_+ + \mathbf{b}_- = \mathbf{0}$$

indicating that contact forces on the two parts at a contact must be equal and opposite, while $\mathbf{b}_0$ must satisfy

$$\mathbf{b}_0 = \mathbf{0}.$$

To summarize, the test to determine whether a COR is I is

$$\begin{aligned} \text{find} \quad & \mathbf{a} \in \mathbb{R}^{8n} \\ & \mathbf{b} \in \mathbb{R}^{2mn} \\ \text{such that} \quad & S\mathbf{a} - P\mathbf{b} = \mathbf{0} \\ & C\mathbf{a} = [1 \ldots 1]^T \\ & \mathbf{a} \geq \mathbf{0} \\ & \mathbf{b}_+ + \mathbf{b}_- = \mathbf{0} \\ & \mathbf{b}_+ \geq \mathbf{0} \\ & \mathbf{b}_0 = \mathbf{0}. \end{aligned} \tag{5}$$

If there is no solution to this linear constraint satisfaction problem, the motion is labeled I.

The I test has $8^n + 2mn$ design variables and $3n + n + 8^n + 2mn$ total constraints. There are at least $3n + n$ equality constraints and at least 8^n inequality constraints. The remaining $2mn$ constraints on $\mathbf{b}$ are divided among inequality constraints for contacts involving only one part ($\mathbf{b}_+ \geq \mathbf{0}$) and equality constraints for contacts involving adjacent parts ($\mathbf{b}_+ + \mathbf{b}_- = \mathbf{0}$) and contacts not acting on a given part ($\mathbf{b}_0 = \mathbf{0}$). We formulate the linear constraint satisfaction problem as a linear program with a zero objective function and solve it using Matlab's `linprog` function which implements a primal-dual interior point method. This computation is done offline.

B. Testing for Stability Consistent With All Support Distributions

To determine if an assembly of n parts falls in category P under a given pushing motion, we must guarantee that pushing wrenches can be generated that yield all possible combinations of support wrenches in the n parts' support wrench regions. To test this property, however, it is sufficient to test if pushing wrenches can be generated to yield each of the 8^n combinations of support wrenches taken from the corners of the support wrench regions. (In other words, for each part i, the support weight vector $\mathbf{a}^i$ is one of $[1,0,0,0,0,0,0,0]^T$, $[0,1,0,0,0,0,0,0]^T, \ldots, [0,0,0,0,0,0,0,1]^T$.) This holds due to the convexity of the constraints placed on the design vector $\mathbf{b}$ by the contact inequality constraints $\mathbf{b}_+ \geq \mathbf{0}$, the contact equality constraints $\mathbf{b}_+ + \mathbf{b}_- = \mathbf{0}$, and the linear force balance equality constraints. More precisely, if there is a solution to the pushing wrench vector $\mathbf{b}_1$ for a support weight vector $\mathbf{a}_1$ and a solution $\mathbf{b}_2$ for a support weight vector $\mathbf{a}_2$, then a problem with a support weight vector $t\mathbf{a}_1 + (1-t)\mathbf{a}_2$, $0 \leq t \leq 1$ is solved by a feasible pushing wrench vector $t\mathbf{b}_1 + (1-t)\mathbf{b}_2$. By induction, it suffices to test for solutions at the extremes of the $\mathbf{a}$ region in its $3n$-dimensional space.

We form 8^n linear constraint satisfaction problems like the one described above, except that the $C\mathbf{a}$ constraint is replaced by an equality constraint on $\mathbf{a}$ choosing one of the 8^n extreme points of the support wrench regions (i.e., $\mathbf{a}$ are no longer design variables). If for each of the 8^n problems there exists a $\mathbf{b}$ that solves it, then the motion is labeled P.

In practice, we form the 8^n linear constraint satisfaction problems for a P test into a single problem with $8^n(2mn)$ design variables and a constraint matrix with the 8^n sets of constraints

on $\mathbf{b}$ in block diagonal form. This amounts to $8^n(3n + 2mn)$ constraints.

C. Testing for Stable Translation Directions

Due to convexity arguments, it can be shown that the set of translation directions labeled P is either: 1) empty; 2) two discrete and opposing directions; or 3) a single connected set on the unit circle of translation directions. In the first case, no pushing motions are labeled P. In the second case, only the two opposing translation directions are labeled P; no pushes with a rotational component are labeled P. In the third case, the full set of pushing motions labeled P is a single connected set in the twist space. These motions can be plotted on the unit velocity sphere $\{\mathbf{v}|v_x^2 + v_y^2 + (\ell\omega_z)^2 = 1\}$, where ℓ is an arbitrary length scale relating translational and rotational velocities. In these plots the included segment of the equator represents the translation directions labeled P (e.g., Fig. 10).

Testing if a translation direction is labeled P is far simpler than testing a general pushing direction including rotation, as the uncertainty in each part's support friction wrench vanishes. Let the translation velocity be written (d_x, d_y). Then, the support wrench at part i is proportional to $f^i_{\max}[d_x, d_y, 0]^T$, where $f^i_{\max} = \mu^i_s m^i g$ is the support friction force magnitude during translation. Call this wrench $\mathbf{f}^i$. Let $\mathbf{f} = \left[(\mathbf{f}^1)^T \ldots (\mathbf{f}^n)^T\right]^T$ be the $3n$ column vector obtained by stacking the $\mathbf{f}^i$.

To find the set of stable translation directions, we can test all of the translations on the unit circle $d_x^2 + d_y^2 = 1$. As this is not a linear constraint, we turn the problem into a set of linear programming problems by testing translation directions on the boundary of the square $\{(d_x, d_y)|\ |d_x| \leq 1, |d_y| \leq 1\}$. For example, choose the edge of the square $d_x = 1, -1 \leq d_y \leq 1$. Solving the linear program

$$\begin{aligned}
\text{find} \quad & d_y \\
& \mathbf{b} \in \mathbb{R}^{2mn} \\
\text{minimizing} \quad & d_y \\
\text{such that} \quad & \mathbf{f} - P\mathbf{b} = \mathbf{0} \\
& \mathbf{b}_+ + \mathbf{b}_- = \mathbf{0} \\
& \mathbf{b}_+ \geq \mathbf{0} \\
& \mathbf{b}_0 = \mathbf{0} \\
& d_y \leq 1 \\
& d_y \geq -1
\end{aligned}$$

where P and $\mathbf{b}$ are as defined in (5), we find either no solution (no translation direction of the form $(1, -1 \leq d_y \leq 1)$ is stable) or a possible boundary of the P translation directions. For this same edge of the (d_x, d_y) square, we can solve a similar program except maximizing d_y. We repeat these two tests for the other three edges of the square, maximizing and minimizing d_x or d_y as appropriate to the edge. After solving these eight linear programs, we have found a (possibly empty) set of P translations. If the set is empty, then no pushing motions are labeled P (case 1 above). If the set consists of just two antipodal directions, then we have case 2 above. Otherwise, the stable translation directions are given by the convex hull of the solutions to the eight linear programming problems.

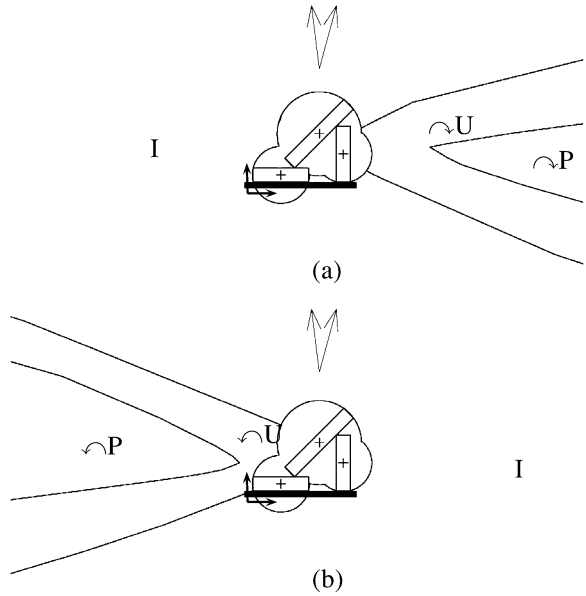

Fig. 9. These plots show I, U, and P regions of (a) clockwise and (b) counterclockwise CORs for a three-part assembly. Stable translation directions are also shown. The pushing friction coefficient is 0.5 at all contacts. The support friction coefficient is the same for all parts, and the ratio of the mass of the longer part to each of the other parts is 10/7.

VI. Results

The examples in Figs. 9 and 11 were analyzed by testing CORs drawn from an adaptive grid. The goal is to find the boundary of the P region by testing individual points. For each rotation sense (clockwise and counterclockwise), a coarse grid was first tested to find the approximate boundary between CORs labeled I and CORs not labeled I using the test given in Section V-A. No CORs inside disks approximating the parts were tested. Progressively finer grids were used to home in on the boundary. A similar procedure was followed to identify the P region using the test of Section V-B. Finally, stable translation directions were determined using the algorithm in Section V-C.

It should be kept in mind that the pairs of P regions identified in the two examples actually correspond to single connected regions in the twist space. We plot these connected regions using the data from Figs. 9 and 11 and the results of the stable translation test in Figs. 10 and 12, respectively. The COR P regions are connected at CORs at infinity (translations). To plot the CORs labeled P on the unit velocity sphere, we generally choose an origin in the plane somewhere on the parts or the pusher so that CORs close to the parts have a high rotational component. Since we can choose a length scale ℓ arbitrarily, we choose ℓ to put the COR labeled P closest to the origin at approximately 40° latitude or 65 percent of the $\ell\omega_z$ axis for good visibility on the sphere. In Figs. 9 and 10, the two smaller rectangles are 400 units long, and the origin for CORs is at the lower left corner of the horizontal rectangle. So the closest P COR is the one at the point of the counterclockwise P region. We chose the length scale $\ell = 188$ to put this point at approximately 40° latitude in Fig. 10. Similarly, in Figs. 11 and 12, the right triangle has legs that are 200 units in length and the origin for CORs is at the corner of the pusher. The closest COR is the one at the point of

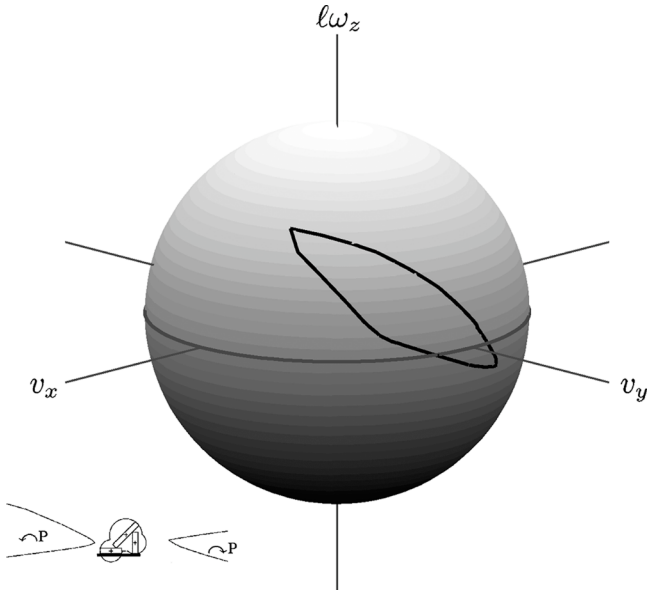

Fig. 10. Plot of the twists labeled P for the three-part assembly in Fig. 9. The inset shows the same data as CORs.

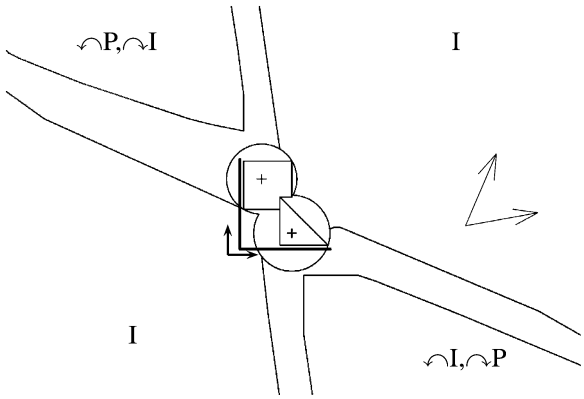

Fig. 11. Combined plot of I and P COR regions for a two-part assembly. Stable translation directions are also shown. One part rests in an interior corner of the other part. The pushing contacts are frictionless, meaning that CORs labeled P are guaranteed to be stable. The support friction coefficient is the same for both parts, and the ratio of the mass of the triangular part to the other part is 5/9.

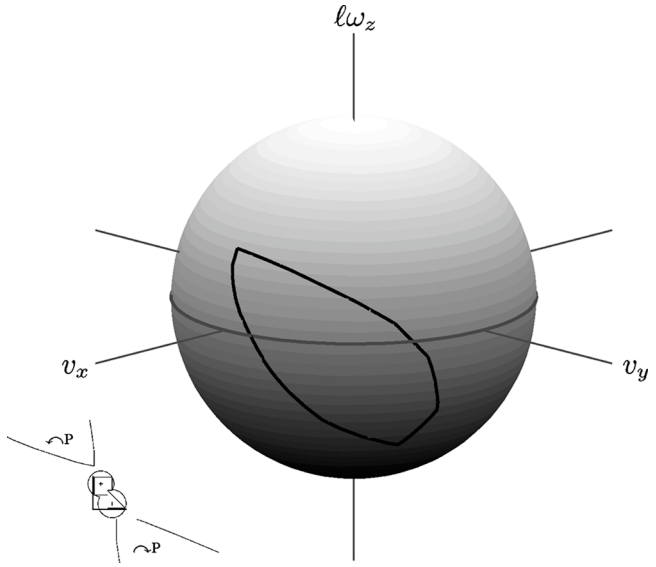

Fig. 12. Plot of the twists labeled P for the two-part assembly in Fig. 11. The inset shows the same data as CORs.

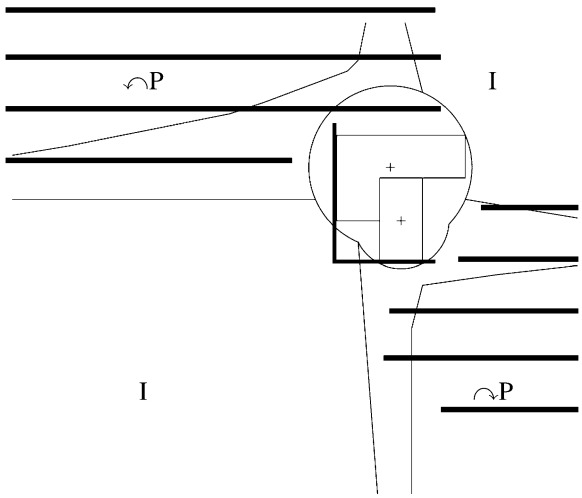

Fig. 13. Predicted and actual results for a two-part experiment. The dark bands are stable CORs. The stable CORs at the top left are counterclockwise and the ones at the bottom right are clockwise. The analysis was done with frictionless contacts, but the actual contact friction coefficient was estimated to be $\mu = 0.2$.

the clockwise P region. We chose the length scale $\ell = 235$ to put this point at approximately -40° latitude in Fig. 12.

The U regions separating P and I regions are due to the uncertainty in the support distribution. As CORs move off to infinity, the boundaries of the P and I regions become parallel, meaning that CORs at infinity (translational motion of the assembly) are uniquely marked as either P or I. This is another way of saying that the uncertainty in the support wrenches goes to zero. For a COR sufficiently far from the assembly, we can approximately model the support distribution for each part as concentrated at the CM and solve a single problem of the form in Section V-B, instead of 8^n problems, to test if a motion is P.

We use Matlab's `linprog` function to solve the constraint satisfaction problems. In the three-part example above, a typical I test for a given COR takes approximately 0.2 s on a 2.8-GHz Pentium 4 PC. Finding stable translation directions takes less than 1 s. A typical P test for a COR takes approximately 3 s. Recalling the sizes of the parts given earlier, we used an adaptive grid to get a resolution of 25 units $\times$ 25 units. The plots in Figs. 9 and 11 took approximately 3.5 and 66 min of computation, respectively. The latter example took longer partly due to more interdependence of the pushing contact constraints and partly due to testing a larger grid of CORs.

VII. Experiment

Fig. 13 shows the predicted and actual results of an experiment with two parts. The parts were placed on a constantly turning turntable and allowed to rest against a stationary right-angle pusher. This is quasi-statically equivalent to a moving pusher rotating about a COR at the center of a stationary turntable. The parts were made from 2.5-cm-thick plexiglass. The small part measured 8 cm $\times$ 4 cm and the large part measured 12 cm $\times$ 8 cm. A binary search was used to find

the transition between stable and unstable CORs along each line of CORs. If the parts did not move relative to the pusher or each other for one complete rotation of the table then that COR was deemed stable.

The algorithms in Sections V-A and V-B were used to determine the I and P regions for the parts. In Fig. 13, the predictions were made with frictionless contacts, but the actual contact friction coefficient was estimated to be $\mu = 0.2$. If the experimental parts were indeed frictionless, then every COR in the P region should be experimentally stable. We hypothesize that these CORs remain stable for larger coefficients of friction. We found that almost all CORs we tested in the P region were indeed stable. We presume that the exceptions (bottom right of Fig. 13) were due to the table not being very flat near the edges, which upset the assembly. Note that the stable CORs that appear in the I region do not contradict our theory because the pusher–part and part–part coefficients of friction are greater than zero.

There were various failure modes for unstable CORs. In some cases, the parts remained fixed relative to one another, but slid along one or the other of the two pusher edges. In some cases, the assembly maintained its shape but rotated around one of the outside corners in contact with the pusher. And in some cases the parts separated from one another. Videos of stable and unstable pushing demonstrations can be found on the Web.[1] The results in Fig. 13 were obtained on a turntable, but the videos show an adjustable, moving fixture pushing the parts on a fixed surface.

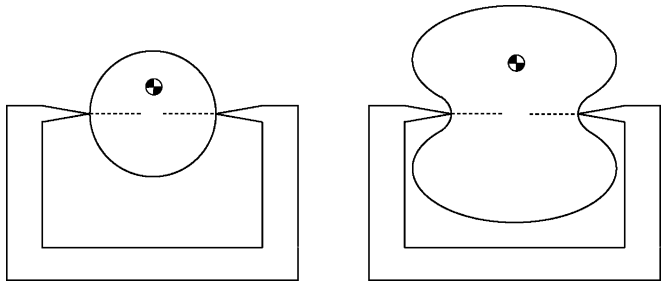

Fig. 14. Same pusher and two different parts with the same contact locations and contact normals. The assembly on the right will be stable for any motion of the pusher because of kinematic considerations.

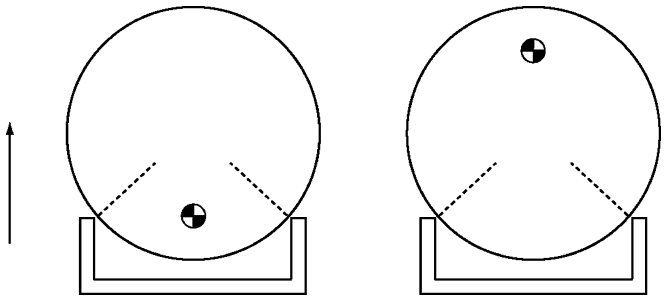

Fig. 15. Translational pushing direction indicated is labeled P for both examples, where the pushing contacts are frictionless. The disk on the left will return to its initial configuration relative to the pusher for small positional perturbations, while the disk on the right will not. In neither case is the support wrench for translation in the interior of the pushing wrench cone.

VIII. Discussion and Conclusion

This paper describes algorithms for deciding whether a pushed assembly is or is not guaranteed to fall apart. Precisely, these algorithms label a given pushing motion P (which means any force necessary to preserve the assembly can be generated by the pushing contacts), I (pushing forces cannot preserve the assembly), or U (pushing forces may or may not be able to preserve the assembly). Pushing motions are labeled U due to indeterminacy of the support friction wrench at each part. This paper has described a method for bounding this indeterminacy. These bounds are conservative; tighter bounds would allow shrinking the set of motions labeled U.

Motions labeled P are guaranteed to be stable if the pusher–part and part–part contacts are frictionless. If these contacts are not frictionless, stability is a consistent solution for motions labeled P, but other solutions may exist due to the possibility of multiple solutions to rigid-body mechanics problems with Coulomb friction. Showing that no other motion is possible potentially requires testing a number of contact modes exponential in the number of contacts (i.e., slipping left or right, sticking, or breaking free at each contact) [2], [16]. While it seems apparent in many cases, it has not been proven that increasing pushing friction cannot make a previously guaranteed stable motion unstable.

This paper uses a first-order model of point contact: contacts are defined completely by their location and contact normal. Higher order contact geometry (e.g., local relative curvature of the parts) is not considered. As shown by Rimon and Burdick [23], however, curvature may play an important role in determining the behavior of the system. Fig. 14 shows two sets of first-order-equivalent pushing contacts. If the pushing friction coefficient is zero, the pushing wrench cones have empty interiors and do not include forces through the CM. The algorithms in this paper would declare that most motions are I and none are P. Nonetheless, it is clear that all pushing motions will be stable for the situation on the right, purely by kinematic considerations, while this is not the case for the situation on the left. Thus, pushing motions labeled I in this paper might actually be stable depending on higher order contact geometry.

Finally, in this paper we have been using the word "stable" to mean that the assembly is preserved for a specific nominal pushing motion and no perturbations. There is no notion of stability to perturbations in either the support wrenches or the configuration of the assembly. Stability in the former case could be defined as the situation where all possible support wrenches are contained in the *interior* of the possible pushing wrenches. This is equivalent to a pushing motion being in the interior of the P set, and is a trivial addition to the analysis in this paper. Stability in the latter case is more subtle, depending on the local contact geometry of parts in the assembly (see Fig. 15). We have observed that an assembly being pushed in a stable direction will often reassemble after small positional perturbations, but we have not characterized this phenomenon.

Acknowledgment

The authors would like to thank the anonymous reviewers for their helpful comments and suggestions.

[1][Online]. Available: http://www.ieeexplore.ieee.org or http://www.lims.mech.northwestern.edu/~lynch/research/videos/.

REFERENCES

[1] D. Balkcom and J. C. Trinkle, "Computing wrench cones for planar contact tasks," *Int. J. Robot. Res.*, vol. 21, no. 12, pp. 1053–1066, 2002.

[2] D. Baraff, Determining frictional inconsistency is NP-complete Dept. Comput. Sci., Cornell Univ., Ithaca, NY, 90-1112, Apr. 1990.

[3] D. Baraff, R. Mattikalli, and P. Khosla, "Minimal fixturing of frictionless assemblies: Complexity and algorithms," *Algorithmica*, vol. 19, no. 1/2, pp. 4–39, 1997.

[4] J. Bernheisel and K. Lynch, "Stable transport of assemblies: Pushing stacked parts," in *Proc. IEEE/RSJ Int. Conf. Intell. Robots Syst.*, 2003, pp. 3180–3185.

[5] J. D. Bernheisel and K. M. Lynch, "Stable transport of assemblies: Pushing stacked parts," *IEEE Trans. Autom. Sci. Eng.*, vol. 1, no. 2, pp. 163–168, Oct. 2004.

[6] P. E. Dupont, "The effect of Coulomb friction on the existence and uniqueness of the forward dynamics problem," in *Proc. IEEE Int. Conf. Robot. Autom.*, Nice, France, 1992, pp. 1442–1447.

[7] L. Han, J. C. Trinkle, and Z. Li, "Grasp analysis as linear matrix inequality problems," in *Proc. IEEE Int. Conf. Robot. Autom.*, 1999, pp. 1261–1268.

[8] K. Harada, M. Kaneko, and T. Tsuji, "Rolling based manipulation for multiple objects," *IEEE Trans. Robot. Autom.*, vol. 16, no. 5, pp. 457–468, Oct. 2000.

[9] K. Harada, J. Nishiyama, Y. Murakami, and M. Kaneko, "Pushing multiple objects using equivalent friction center," in *Proc. IEEE Int. Conf. Robot. Autom.*, 2002, pp. 2485–2491.

[10] P. Lötstedt, "Coulomb friction in two-dimensional rigid body systems," *Zeitschrift für Angewandte Mathematik und Mechanik*, vol. 61, pp. 605–615, 1981.

[11] K. M. Lynch, "The mechanics of fine manipulation by pushing," in *Proc. IEEE Int. Conf. Robot. Autom.*, Nice, France, 1992, pp. 2269–2276.

[12] K. M. Lynch and M. T. Mason, "Stable pushing: Mechanics, controllability, and planning," *Int. J. Robot. Res.*, vol. 15, no. 6, pp. 533–556, Dec. 1996.

[13] Y. Maeda and T. Arai, "A quantitative stability measure for graspless manipulation," in *Proc. IEEE Int. Conf. Robot. Autom.*, 2002, pp. 2473–2478.

[14] Y. Maeda, H. Kijimoto, Y. Aiyama, and T. Arai, "Planning of graspless manipulation by multiple robot fingers," in *Proc. IEEE Int. Conf. Robot. Autom.*, 2001, pp. 2474–2479.

[15] M. T. Mason, "Mechanics and planning of manipulator pushing operations," *Int. J. Robot. Res.*, vol. 5, no. 3, pp. 53–71, Fall, 1986.

[16] ——, *Mechanics of Robotic Manipulation*. Cambridge, MA: MIT Press, 2001.

[17] M. T. Mason and J. K. Salisbury, *Robot Hands and the Mechanics of Manipulation*. Cambridge, MA: MIT Press, 1985.

[18] R. Mattikalli, D. Baraff, and P. Khosla, "Finding all stable orientations of assemblies with friction," *IEEE Trans. Robot. Autom.*, vol. 12, no. 2, pp. 290–301, Apr. 1996.

[19] R. Mattikalli, D. Baraff, P. Khosla, and B. Repetto, "Gravitational stability of frictionless assemblies," *IEEE Trans. Robot. Autom.*, vol. 11, no. 3, pp. 374–388, Jun. 1995.

[20] H. Mayeda and Y. Wakatsuki, "Strategies for pushing a 3D block along a wall," in *Proc. IEEE/RSJ Int. Conf. Intell. Robots Syst.*, Osaka, Japan, 1991, pp. 461–466.

[21] H. Mosemann, F. Roehrdanz, and F. Wahl, "Stability analysis of assemblies considering friction," *IEEE Trans. Robot. Autom.*, vol. 13, no. 6, pp. 805–813, Dec. 1997.

[22] M. A. Peshkin and A. C. Sanderson, "The motion of a pushed, sliding workpiece," *IEEE J. Robot. Autom.*, vol. 4, no. 6, pp. 569–598, Dec. 1988.

[23] E. Rimon and J. W. Burdick, "New bounds on the number of frictionless fingers required to immobilize planar objects," *J. Robot. Syst.*, vol. 12, no. 6, pp. 433–451, 1995.

[24] J.-C. Trinkle, "On the stability and instantaneous velocity of grasped frictionless objects," *IEEE Trans. Robot. Autom.*, vol. 8, no. 5, pp. 560–572, Oct. 1992.

[25] Y. Yu, K. Fukuda, and S. Tsujio, "Computation of grasp internal forces for stably grasping multiple objects," in *Proc. IEEE Int. Symp. Comput. Intell. Robot. Autom.*, 2001, pp. 17–22.

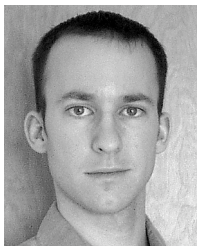

Jay D. Bernheisel (S'01) received the B.S. and M.S. degrees in mechanical engineering from the Rose–Hulman Institute of Technology, Terre Haute, IN, in 1996 and 1997, respectively. He is currently working toward the Ph.D. degree in mechanical engineering at the Laboratory for Intelligent Mechanical Systems, Northwestern University, Evanston, IL.

Before coming to Northwestern in 2001, he was a Flight Test Engineer in the U.S. Air Force. His research interests include stable transport of assemblies and self-assembly.

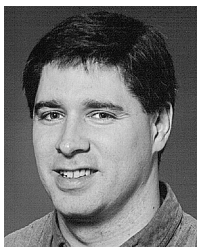

Kevin M. Lynch (S'89–M'96–SM'05) received the B.S.E. degree in electrical engineering from Princeton University, Princeton, NJ, in 1989, and the Ph.D. degree in robotics from Carnegie Mellon University, Pittsburgh, PA, in 1996.

He is an Associate Professor of Mechanical Engineering with Northwestern University, Evanston, IL, where he co-directs the Laboratory for Intelligent Mechanical Systems. Before moving to Northwestern in 1997, he spent a year and a half as an NSF/STA Postdoctoral Fellow with the Mechanical Engineering Laboratory, Tsukuba, Japan, where he also taught at the University of Tsukuba. His research interests include robot manipulation planning, motion planning and control for underactuated mechanical systems, self-organizing systems, and human–robot systems.